PHYSICAL REVIEW LETTERS

VOLUME 37 | 9 AUGUST 1976 | NUMBER 6

Detection of $\bar{\nu}_e$-e Scattering*

F. Reines, H. S. Gurr, and H. W. Sobel

Department of Physics, University of California, Irvine, California 92717

(Received 27 May 1976)

The reaction $\bar{\nu}_e + e^- \rightarrow \bar{\nu}_e + e^-$ has been observed using a 15.9-kg plastic scintillation target in a composite plastic-NaI-liquid detector exposed to a $\bar{\nu}_e$ flux of 2.2×10^{13} cm^{-2} sec^{-1} from an 1800-MW fission reactor. Tests rule out a reactor-associated signal produced by inverse β decay, neutrons, or gamma rays. The measured cross section is consistent with $V-A$ and the Weinberg model with parameter $\sin^2\theta_W = 0.29 \pm 0.05$.

We report detection of the elastic scattering reaction,

$$\bar{\nu}_e + e^- \rightarrow \bar{\nu}_e + e^- . \tag{1}$$

The observation of this purely leptonic reaction with properties important to the weak interaction and astrophysics is the culmination of experimental efforts[1] which began in 1935 when the then upper bounds were used to deduce limits on a possible neutrino magnetic moment. In the ensuing years $V-A$ theory replaced the magnetic moment as the explanation for $\bar{\nu}_e$-e^- elastic scattering, and declared the magnetic moment to be zero.[2] It was shown in turn that the $V-A$ interaction which accounted for charge-changing inverse β decay and muon decay suffered from different divergence difficulties when applied to the elastic-scattering reaction.[3] More recently, the Salam-Ward, Weinberg, and other theories have been developed.[4] We present our results to exhibit the allowed range of vector and axial-vector coupling constants for comparison with the general class of theories involving these couplings. The history of this experiment is largely an account of the successful identification and reduction of backgrounds. In the present paper we deal explicitly with reactor-associated backgrounds.

The apparatus employed is shown in Fig. 1. It consists of a 15.9-kg plastic scintillation detector segmented into sixteen optically isolated ele-

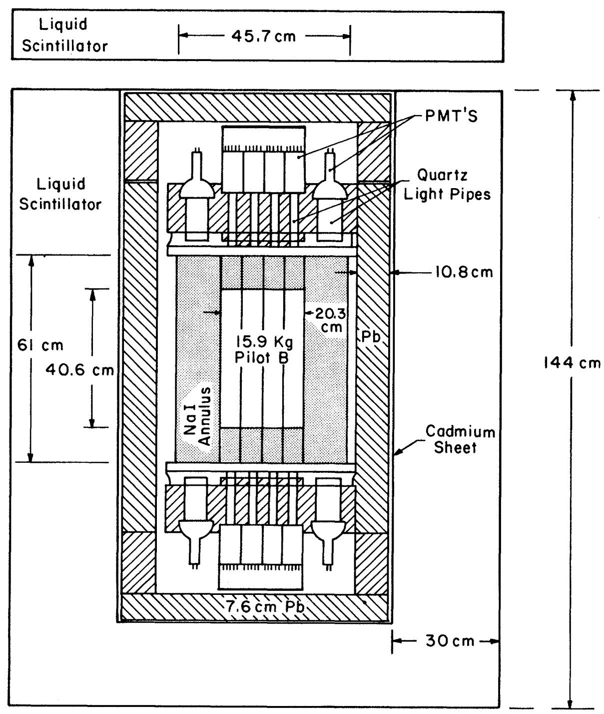

FIG. 1. Schematic of detector showing plastic target region, NaI light pipes, and annulus anticoincidence encased in lead, cadmium absorber, and liquid scintillation anticoincidence detector.

TABLE I. Summary of elastic scattering data (events/day).

Energy bin (MeV)	Reactor on	Reactor off	Stability error	Reactor associated rate	Standard deviations from zero
1.5 – 2.0	30.6 ± 0.8	26.9 ± 0.7	± 0.60	3.7 ± 1.3	2.8
2.0 – 2.5	10.5 ± 0.5	9.1 ± 0.4	0.38	1.4 ± 0.8	1.8
2.5 – 3	4.0 ± 0.2	3.2 ± 0.2	0.17	0.8 ± 0.4	2.2
3.0 – 3.5	1.5 ± 0.2	0.6 ± 0.1	0.08	0.9 ± 0.2	4.3
3.5 – 4	0.54 ± 0.09	0.35 ± 0.08	0.03	0.2 ± 0.1	1.6
4.0 – 4.5	0.40 ± 0.08	0.21 ± 0.06	0.01	0.2 ± 0.1	1.6
1.5 – 3	45.1 ± 1.0	39.2 ± 0.9	± 0.60	5.9 ± 1.4	4.1
3 – 4.5	2.4 ± 0.19	1.2 ± 0.14	0.08	1.2 ± 0.25	4.8
	(64.6 day live time)	(60.7 day live time)			

ments totally enclosed in a 300-kg NaI scintillation detector. The plastic is viewed through NaI light pipes, and signals from the NaI and plastic are distinguished by pulse shape. The NaI annulus is divided into six parts each separately viewed by photomultiplier tubes. The entire composite detector is in turn enclosed in a Pb-Cd shield and immersed in a 2200-l liquid scintillation detector. Further lead, concrete, and water shielding complete the assembly.

Pulse heights and timing information were displayed on an oscilloscope screen and photographed. Minimal trigger constraints were imposed to allow subsequent measurement not only of the elastic scattering reaction (1), but of the inverse β reaction,

$$\bar{\nu}_e + p \to n + e^+ , \qquad (2)$$

and various backgrounds. An elastic-scattering event should produce a count most frequently in one plastic scintillator element unaccompanied by pulses in other adjacent plastic elements, the surrounding NaI, or liquid scintillator. Further, such events should not be associated as either the first or second pulse in delayed coincidence with pulses anywhere in the system. The rate of events associated with the reactor and meeting these and other background-reducing criteria is a measure of the elastic-scattering reaction. A summary of the elastic-scattering data is shown in Table I. The energy calibration was made with a ^{208}Tl (2.6 MeV) γ-ray source periodically introduced into the inner lead shield. Concurrent gain stability and efficiency checks were made by using the internal contaminant ^{214}Bi β spectrum (end point 3.2 MeV) identified by means of a delayed coincidence with an associated α particle from its ^{214}Po daughter.

Table I exhibits a reactor-associated rate in each of six separate energy bins. Lumping the data into two independent energy bins 1.5–3 and 3–4.5 MeV, one observes that each exhibits an effect >4 standard deviations. We believe this to be clear evidence for a reactor-associated signal. We now demonstrate that this signal is not due to inverse β decay, reactor-associated neutrons, or γ rays.

Inverse β-decay background.—The inverse β-decay reaction which occurs in our plastic detector at a rate of 200/d is identified by a prompt positron annihilation pulse and/or delayed neutron capture. This reaction can, because of inefficiencies in neutron and annihilation γ-ray detection, masquerade as a single electron so producing a background for elastic scattering. These rates are $<2\%$ and $<3\%$ of the reactor-associated signals in the energy ranges 1.5–3 and 3–4.5 MeV, respectively.

The argument leading to those results is as follows: (1) For each delayed coincidence from Reaction (2), two 0.5-MeV positron-annihilation γ rays are produced. A count was made of the reactor-associated number of such triggers in which zero, one, or two γ rays were observed in the segmented NaI annulus. This yielded the single-γ-ray detection efficiency $\eta_\gamma \geq 0.96 \pm 0.04$. (2) For each reactor-associated event in which two 0.5-MeV γ's were seen in the NaI annulus, a delayed neutron pulse was sought. This yielded the neutron-detection efficiency $\eta_n = 0.76 \pm 0.07$.

Accordingly, the probability of a background count from inverse β decay is

$$P = (1-\eta_n)(1-\eta_\gamma)^2 = (4 \pm 8)\times 10^{-4},$$

i.e., $P \approx 10^{-3}$ at one standard deviation. Multiplying this probability by the predicted inverse β

TABLE II. Plastic/annulus ratios and inferred backgrounds (1.5–4.5 MeV). Reactor-associated rates for the plastic and annulus are, respectively, $\Delta P = 7.1 \pm 1.5\ \text{day}^{-1}$, $\Delta A = (-1.6 \pm 2.6)\times 10^2\ \text{day}^{-1}$.

Conditions	$(\Delta P/\Delta A)_b$	Inferred background rate per day in plastic (ΔP_b)	Background/signal $\Delta P_b/\Delta P$
Shield doors open	$(0.5\pm 6.6)\times 10^{-4}$	$(-1\pm 10)\times 10^{-2}$	$(-1\pm 14)\times 10^{-3}$
γ ray source	$(1.4\pm 0.2)\times 10^{-4}$	$(-2\pm 4)\times 10^{-2}$	$(-3\pm 5)\times 10^{-3}$
Neutron source	$(1.4\pm 0.2)\times 10^{-3}$	$(-2\pm 4)\times 10^{-1}$	$(-3\pm 5)\times 10^{-2}$

rate in the two energy bins used, we obtained the cited results. Monte Carlo calculations gave results consistent with these.

γ-ray and neutron background.—Several classes of tests eliminated γ rays and neutrons as the source of the reactor-associated signal.

(1) One class employed the NaI annulus anticoincidence detector to set limits on the background seen by the plastic target detector. We measured "plastic-to-annulus ratios," $\Delta P/\Delta A$, with a variety of sources to determine the background rejection efficiency of our detector. Such ratios are used to estimate various reactor-associated backgrounds in the target not eliminated by the NaI and liquid anticoincidences.

We have determined $\Delta P/\Delta A$ with (i) the background spectrum produced when we removed about $\frac{1}{3}$ of our external shielding (by opening the composite lead and water shield doors), (ii) a ^{208}Tl γ source, and (iii) a Pu-Be neutron source which gives capture gammas.

The reactor-associated annulus rate with maximal shielding, ΔA, is then multiplied by the plastic-to-annulus anticoincidence factor $(\Delta P/\Delta A)_b$ to arrive at a limit on the background plastic rate ΔP_b. The result is then compared with the actual plastic signal ΔP. Table II lists the values of $(\Delta P/\Delta A)_b$, ΔA, ΔP_b, and $\Delta P_b/\Delta P$ inferred from these tests. Since the differential shielding technique most accurately reproduces the actual constituents and energy spectrum of the reactor-associated background, the preferred upper limit for $\Delta P_b/\Delta P$ is 0.014.

(2) The second class of tests, summarized in Table III, independently demonstrates the small contribution of γ rays and neutrons. This is based on the fact that electron recoils occur mainly in a single plastic element whereas backgrounds will occur primarily in multiple elements. We use the ratio of the reactor-associated rate occurring in one element (S) to that occurring in more than one element (M) of the plastic detector. Then, if $S_0 = S_e + S_b$ and $M_0 = M_e + M_b$,

$$\frac{S_b}{S_e} = \frac{1-(S_0/M_0)(M_e/S_e)}{(S_0/M_0)(M_b/S_b)-1}, \qquad (3)$$

where the subscripts 0, e, b refer, respectively, to the total observed data, electron contribution, and background contribution. The ratio M_e/S_e (≈ 0.22) is calculated using the range of scattered electrons (1.5–4.5 MeV) and the geometry of the plastic detector. The ratio M_b/S_b is given in Table III for two different background sources.

An additional independent argument can be made to rule out backgrounds from neutron scattering on protons in the plastic scintillator: The neutron spectrum associated with the reactor is of limited energy (< 10 MeV) and the scintillator is inefficient in producing light from slow protons.

These two classes of tests are seen to limit the reactor-associated signal from other than elastic scattering to well under 10%.

Having demonstrated the existence of an elastic-scattering signal,[5] we now compare the results with some theoretical possibilities. The

TABLE III. Multiple/single ratios and inferred backgrounds (1.5–4.5 MeV).

Condition	M/S	Background/signal $(S_b S_e)$
Observed signal	0.18 ± 0.17	...
γ ray sources (^{208}Tl, ^{60}Co)	6.3 ± 1.6	-0.01 ± 0.03
Neutron source	1.3 ± 0.2	-0.04 ± 0.15

most general statement of the differential elastic scattering cross section, $d\sigma/dE$, for a monoenergetic $\bar{\nu}_e$ in terms of vector and axial-vector coupling is[6]

$$\frac{d\sigma}{dE}=\frac{G^2 m_e}{2\pi}\left\{(C_V+C_A)^2+(C_V-C_A)^2\left(1-\frac{E}{E_\nu}\right)^2+\frac{m_e E}{E_\nu^2}(C_A^2-C_V^2)\right\}, \tag{4}$$

where $G^2 m_e/2\pi = 4.1\times 10^{-45}$ cm^2 MeV^{-1}, E is the kinetic energy of recoil electron, and E_ν is the energy of incident $\bar{\nu}_e$. For $V-A$, $C_V=-C_A=1$; for Weinberg, $C_V=\frac{1}{2}+2x$, $C_A=-\frac{1}{2}$, with $x=e^2/g^2=\sin^2\theta_W$. Folding this differential cross section with the reactor $\bar{\nu}_e$ spectrum,[7] the single-element electron containment efficiency, and the detector resolution, and allowing for systematic uncertainties in calibration, we find the results summarized in Fig. 2.

The observed cross sections in the two energy ranges are $\sigma_{\rm expt}=(0.87\pm0.25)\sigma_{V-A}$(1.5 MeV $<E<$ 3.0 MeV), and $\sigma_{\rm expt}=(1.70\pm0.44)\sigma_{V-A}$(3.0 MeV $<E<$ 4.5 MeV). σ_{V-A} lies in the range 10^{-45}–10^{-46} cm^2 (1.5 MeV $<E<$ 4.5 MeV). The observed cross section, though clearly not incompatible with $V-A$, appears to favor the Weinberg model[4] with $x=0.29\pm0.05$.[8]

It is a pleasure to thank the many people who have contributed to this work over the years. Most particularly we express our appreciation to August Hruschka, Thomasina Jones, and our film scanning crew headed by Ann Vitarelli. The Harshaw Chemical Company division under Elmer Stewart rendered invaluable assistance in the construction of the detector. We are grateful to our hosts at the Savannah River Plant of the E. I. DuPont de Nemours Company where these measurements were made.

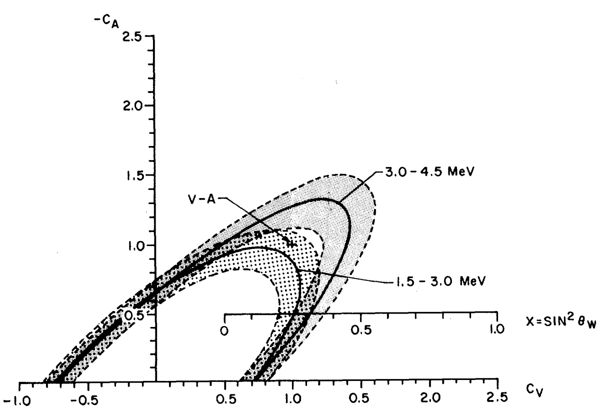

FIG. 2. Values of vector and axial-vector coupling constants permitted by the experiment in regions (a) 1.5–3 MeV and (b) 3–4.5 MeV. The dashed curves are one-standard-deviation limits. $x=\sin^2\theta_W$ is the Weinberg parameter; for region (a) $x=0.26\,^{+0.05}_{-0.06}$, and for (b) $x=0.32\pm0.05$.

*Sponsored by the U. S. Energy Research and Development Administration.

[1]M. E. Nahmias, Proc. Cambridge Philos. Soc. 31, 99 (1935); C. L. Cowan, F. Reines, and F. B. Harrison, Phys. Rev. 96, 1294 (1954); C. L. Cowan and F. Reines, Phys. Rev. 107, 528 (1957); F. Reines, Annu. Rev. Nucl. Sci. 10, 1 (1960); F. Reines and H. S. Gurr, Phys. Rev. Lett. 24, 1448 (1970); H. S. Gurr, F. Reines, and H. W. Sobel, Phys. Rev. Lett. 28, 1406 (1972).

[2]R. E. Marshak and E. C. G. Sudarshan, Phys. Rev. 109, 1860 (1958); R. P. Feynman and M. Gell-Mann, Phys. Rev. 109, 193 (1958); A. Salam, Nuovo Cimento 5, 299 (1957); L. Landau, Nucl. Phys. 3, 127 (1957).

[3]M. Gell-Mann, M. Goldberger, N. Kroll, and F. Low, Phys. Rev. 179, 1518 (1969).

[4]A. Salam and J. C. Ward, Phys. Lett. 13, 168 (1964); S. Weinberg, Phys. Rev. Lett. 19, 1264 (1967); G. 't Hooft, Nucl. Phys. B35, 167 (1971).

[5]We make the assumption that the signal is due to $\bar{\nu}_e$ because it is the only known particle produced in fission or secondary to it which can cause our results.

[6]D. Yu. Bardin, S. M. Bilenky, and B. Pontecorvo, Phys. Lett. 32B, 68 (1970); G. 't Hooft, Phys. Lett. 37B, 195 (1971); H. H. Chen and B. W. Lee, Phys. Rev. D 5, 1874 (1972); L. M. Sehgal, Nucl. Phys. B70, 61 (1974).

[7]F. T. Avignone, III, Phys. Rev. D 2, 2609 (1970).

[8]This value of x is to be compared with $x=0.33\pm0.07$ deduced from neutral-current semileptonic neutrino experiments at accelerators. F. J. Sciulli, private communication.